

AKADÉMIAI KIADÓ



International Review of  
Applied Sciences and  
Engineering

13 (2022) 2, 174–184

DOI:

10.1556/1848.2021.00330

© 2021 The Author(s)

ORIGINAL RESEARCH  
PAPER



# Prediction of the impact of climate change on the thermal performance of walls and roof in Morocco

Yassine Kharbouch\*  and Mohamed Ameer

Energetic Laboratory, University of Abdelmalek Essaâdi, Tetouan, Morocco

Received: June 23, 2021 • Accepted: August 19, 2021

Published online: September 24, 2021

## ABSTRACT

Climate change has become a real challenge in different fields, including the building sector. Understanding and assessing the impact of climate change on building energy performance is still necessary to elaborate new climate-adaptive design measures for future buildings. The building energy consumption for heating and cooling is mainly related to the building envelope thermal performance. In this study, the winter heat loss and summer heat gain indicators are proposed to assess and analyse the potential impact of climate change on opaque building envelope elements for different climate zones in Morocco over the next 40 years. For that purpose, a one-dimensional heat transfer model is used to simulate the heat transfer through the multi-layer structure of the wall/roof. A medium climate change scenario is considered in this study. The results showed that the current average walls and roof summer heat gain is expected to increase of about 19.2–54.3% by the 2060s depending on the climate zone, versus a less important decrease in winter heat loss varies between –10.6 and –20.6%. This paper provides a reliable evaluation of the climate change impact on building envelope thermal performance, which leads to better adjustments in future building envelope designs.

## KEYWORDS

wall, roof, thermal performance, climate change, heat loss, heat gain

## 1. INTRODUCTION

Nowadays, we are living a rapid climate change with all its aspects, including the rise of global temperature (called global warming). This change has begun to appear since the first industrial revolution and has become increasingly important with the expansion of greenhouse emission caused by human activity. The devastating effects of this climate change have set alarm bells ringing all over the world. The United Nations Framework Convention on Climate Change (UNFCCC) that has emanated from the earth summit in 1992, represents the first step in addressing the climate change problem [1]. Five years later, the Kyoto protocol has been adopted by the international community for limiting and reducing greenhouse gas emissions (GHG) [2]. The validity of this protocol ends by 2020, and then will be replaced by the Paris agreement adopted in 2015 that sets a target of limiting global temperature to below 2 °C above the pre-industrial level [3]. Nevertheless, the achievement of this target depends on how far different countries respect their commitments to reduce GHG emissions. On the other side, the scientific community is still engaged in exploring the various future climate scenarios and their implications on various sectors.

The Intergovernmental Panel on Climate Change (IPCC) is the international structure created for studying the different questions relevant to climate change. According to its fifth assessment report [4], the increase of global mean surface temperature by the end of the 21st century, relative to the 1986–2005 period, is likely to be from 0.3 to 1.7 °C under an optimistic GHG emissions scenario, and from 2.6 to 4.8 °C under pessimistic GHG emissions scenario.

\*Corresponding author.

E-mail: [kharbouch.yassine@gmail.com](mailto:kharbouch.yassine@gmail.com)



The building sector has an important role in these remarkable changes due to energy consumption and GHG emissions that it generates. According to IPCC, it represents in 2010, 32% of the final energy and responsible for 19% of energy-related GHG emissions [5]. This energy and the related GHG emissions may be doubled or even tripled by 2050 due to increased access for people in developing countries to adequate housing, electricity, and air-conditioning equipment.

Many researches were conducted to understand the impact of climate changes on building's energy performance in different countries and regions. Frank [6] has found that for the period 2050–2100, the annual cooling energy demand for office buildings could increase by 223–1050%, while the heating energy demand could decrease by 36–58%. The climatic data of 1961–1990 has been considered as baseline data for comparison. Wang et al. [7] have shown that the total heating/cooling energy consumption of Australian five stars houses in five cities, is projected to vary between –23 and 81% in 2050, and between –37 and 193% in 2100, respectively, depending on the selected GHG emissions scenario.

Using the degree-day method, Hamlet et al. [8] have investigated the effects of climate change cooling energy demand in the Pacific Northwest and Washington State in the United States. The authors have found that climate change would increase building cooling energy demand by 174–289% for the 2040s and 371–749% for the 2080s due to the combined effects of increased Cooling Degree Day and increased use of air conditioning. In Brazil, Invidiata and Ghisi [9] have found, by the means of a dynamic building simulation study, that the total heating and cooling energy demand single-family house ( $U_{\text{wall}} = 2.46 \text{ W/m}^{-2} \cdot ^\circ\text{C}$ ;  $U_{\text{roof}} = 1.75 \text{ W/m}^{-2} \cdot ^\circ\text{C}$ ) is expected to rise by 56 – 112% in 2050 and 112 – 185% in 2080. In the coldest city, the annual heating energy demand is expected to decrease by 94% in 2080 due to an increase in the average outdoor temperature. The study has assumed a medium-high growth in future GHG emissions (Scenario A2 [10]). Under the same scenario, Berardi and Jafarpur [11] have assessed the impact of climate change on building heating and cooling energy demand in Canada. Sixteen building prototypes have been simulated. The results showed an average decrease between 18 and 33% of the heating energy demand and an average increase between 15 and 126% of the cooling energy demand by 2070, depending on the baseline climatic data and building typology. On their side, Nematchoua et al. [12] have focused their study on the case of a hospital building located on six islands in the Indian Ocean region. The authors expected an increase in the cooling energy demand of between 60.8 and 95.1% by 2090 depending on the intensity of the climate change scenario. More recently, Rodrigues and Fernandes [13] focused on the impact of climate change in different cities in the south and north of the Mediterranean region by 2050. Based on a medium-high climate change scenario, the authors found that, in most locations, the future increase in building cooling demand is more important than the decrease in heating energy consumption regardless of the choice of the heat transfer coefficient  $U$ -values. The authors have observed, particularly

that the ideal  $U$ -value of the opaque envelope elements for current climate conditions ( $U_{\text{envelope}} = 0.55 \text{ (W/m}^{-2} \cdot ^\circ\text{C)}$ ) would cause, in the future, an increase in the risk of over-heating in Casablanca city in Morocco.

Carrying out a real experimental study on climate change impact is still difficult given that such a study would take many decades. The principal method used for this purpose consists of the building energy simulation method [14]. However, in the most related works, one may observe the inconsistency in the intensity of the impact of climate change on the building. This is due, firstly, to the selected climate zone, climate change scenario, periods being compared, but also to the specificities of each building case study. These specificities include, essentially, the building typology (i.e. building's architecture and size, the occupancy schedule), internal gains, air exchange rate, heating/cooling set points, and the air-conditioning system type. Otherwise, an alternative approach could be used to assess the impact of climate change. It consists of performing an assessment the thermal performance of the building envelope elements instead of the whole building energy performance assessment.

Morocco is a country within the Mediterranean basin that is exposed to important climate change risks [15, 16]. Since the 19th century, the mean outdoor temperature has increased by  $1.4 \text{ }^\circ\text{C}$  and is expected to continue to increase in the future decades. In this work, we are going to study the thermal performance of the opaque building envelope elements (walls and roof) under the climatic conditions of the current and future decades in Morocco. The climate change projection is carried out through the assessment of the winter heat loss and summer heat gain of walls and roof, while considering a medium-rise GHG emissions scenario for the 2020s, 2040s and 2060s periods. We will focus on the different climate zones of Morocco with the consideration of the current building thermal code standards. Furthermore, this study attends also to highlight the possible divergence in the climate change impact intensity in relative to the wall facade and season.

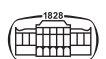
## 2. METHODOLOGY AND MATERIALS

### 2.1. Thermal performance assessment

The thermal performance of the wall/roof is carried out using the heat transmission load. This study will focus on a representative month for winter season (January) and for summer (July). The instantaneous heat loss during the winter season ( $Q_{\text{win-ins}}$ ), and the instantaneous heat gain during the summer season ( $Q_{\text{sum-ins}}$ ) are calculated as follows:

$$Q_{\text{win-ins}}(t) = \int_t^{t+\Delta t} h_{\text{int}} \times (T_{\text{int}}(t) - T_{\text{sur-int}}(t)) dt \quad (1a)$$

$$Q_{\text{sum-ins}}(t) = \int_t^{t+\Delta t} h_{\text{int}} \times (T_{\text{sur-int}}(t) - T_{\text{int}}(t)) dt \quad (1b)$$



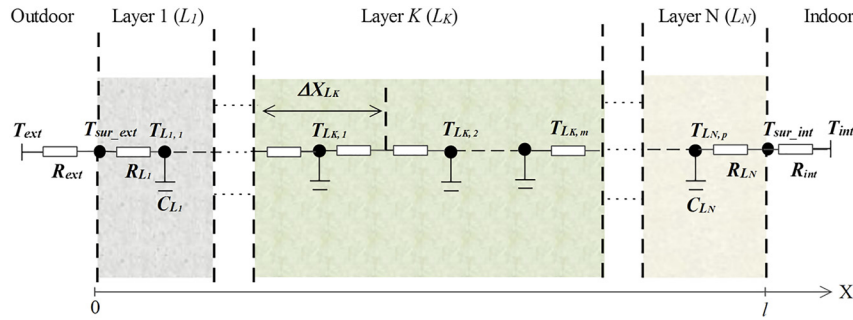


Fig. 1. Space discretization scheme of the wall/roof

where  $h_{int}$ ,  $T_{int}$  and  $T_{sur\_int}$  denote, respectively, the interior heat transfer coefficient, the indoor temperature and the interior surface temperature (see Fig. 1). These instantaneous loads were integrated over the monthly time periods to calculate the monthly winter heat loss  $Q_{win}$  and summer heat gain  $Q_{sum}$ .

**2.2. Heat transfer model and boundary conditions**

The instantaneous variation of the interior surface temperature ( $T_{int}(t)$ ) is needed. For that purpose, we consider a one-dimensional heat transfer model through a multi-layer wall/roof under convective boundary conditions. This model was developed and used previously by Kharbouch et al. [17] to simulate the thermal performance of walls/roof integrated with phase change materials, as well as the conventional walls/roof with constant thermo-physical property material. The contact resistance between different adjacent layers is considered perfect. All layers are considered homogenous and isotropic. For each layer  $L$  of the wall/roof, the energy conservation equation is written as follows:

$$\rho_L c p_L \frac{\partial T_L}{\partial t} = \lambda_L \left( \frac{\partial^2 T_L}{\partial X^2} \right) \text{ for } L = L_1, L_2 \dots L_N. \quad (2)$$

The boundary conditions for Eq. (2) are written as follows:

$$-\lambda_{L_1} \left( \frac{\partial T_{L_1}}{\partial X} \right)_{X=0} = h_{ext} (T_{ext} - T_{L_1}|_{X=0}) \quad (3a)$$

$$-\lambda_{L_N} \left( \frac{\partial T_{L_N}}{\partial X} \right)_{X=l} = h_{int} (T_{L_N}|_{X=l} - T_{int}) \quad (3b)$$

The numerical solution of Eq. (2) with the boundary conditions (Eqs. (3a) and (3b)), has been developed using the resistance-capacitance (RC) approach (see Fig. 1). This approach consists of decomposing each main layer ( $L_K$ ) of the wall/roof into a number of sub-layers  $L_{K,j}$  of thickness  $\Delta X_{L_K}$ . Each sub-layer is characterized by the temperature  $T_{L_{K,j}}$  as shown in Fig. 1. The lumped capacitance ( $C$ ) and the lumped thermal resistance ( $R$ ) per unit area ( $S = 1 \text{ m}^2$ ) of each layer are calculated as follows:

$$C_{L_K} = \rho_{L_K} c p_{L_K} \Delta X_{L_K} S \quad (4a)$$

$$R_{L_K} = \frac{\Delta X_{L_K}}{2 \lambda_{L_K} S} \quad (4b)$$

The energy balance at each internal node is given as follows:

$$C_{L_{1,1}} \frac{dT_{L_{1,1}}}{dt} = \frac{T_{sur\_ext} - T_{L_{1,1}}}{R_{L_{1,1}}} - \frac{T_{L_{1,1}} - T_{L_{1,2}}}{R_{L_{1,1}} + R_{L_{1,2}}} \quad (5a)$$

$$C_j \frac{dT_j}{dt} = \frac{T_{j-1} - T_j}{R_{j-1} + R_j} - \frac{T_j - T_{j+1}}{R_j + R_{j+1}}; j = L_{1,2} \dots L_{N,p-1} \quad (5b)$$

$$C_{L_{N,p}} \frac{dT_{L_{N,p}}}{dt} = \frac{T_{L_{N,p-1}} - T_{L_{N,p}}}{R_{L_{N,p-1}} + R_{L_{N,p}}} - \frac{T_{L_{N,p}} - T_{sur\_int}}{R_{L_{N,p}}} \quad (5c)$$

The energy balance at the outside and inside surface nodes is written as follows:

$$0 = \frac{T_{ext} - T_{sur\_ext}}{R_{ext}} - \frac{T_{sur\_ext} - T_{L_{1,1}}}{R_{L_{1,1}}} \quad (6a)$$

$$0 = \frac{T_{L_{N,p}} - T_{sur\_int}}{R_{L_{N,p}}} - \frac{T_{sur\_int} - T_{int}}{R_{int}} \quad (6b)$$

$R_{int} = (1/h_{int} \cdot S)$  and  $R_{ext} = (1/h_{ext} \cdot S)$  denote, respectively, the external and the internal surface resistance per unit area. They were taken based on the Moroccan standard as follows [18]:  $R_{ext}$  (wall/roof) = 0.04 ( $^{\circ}\text{C}/\text{W}$ ),  $R_{int}$  (wall) = 0.13 ( $^{\circ}\text{C}/\text{W}$ ),  $R_{int}$  (roof) = 0.10 ( $^{\circ}\text{C}/\text{W}$ ).

The resulting system of Eqs. (5) and (6) can be presented in matrix form as follows:

$$\left[ \frac{dT}{dt} \right] = [A] \cdot [T] + [B] \quad (7)$$

where  $[A]$  is the matrix containing the thermal resistance and capacitance, and the matrix  $[B]$  contains the boundary conditions.

The time discretisation of the problem is done using an implicit scheme of the finite difference method. We obtain a tri-diagonal problem of the form  $D \times [T^{\Delta t+t}] = E$ , where  $T^{\Delta t+t}$  is the temperature vector at the time  $t+\Delta t$ ,  $D$  is the tridiagonal matrix, and  $E$  is a known vector corresponding to the previous time step. The Thomas algorithm was applied to the resulting system under the Matlab environment. A time step of the  $\Delta t = 60\text{s}$  is considered.

The developed model is successfully validated against experimental data from Antonopoulos and Democritou [19] as shown in Fig. 2. The experimental protocol of [19] consisted of imposing a periodic temperature wave on the



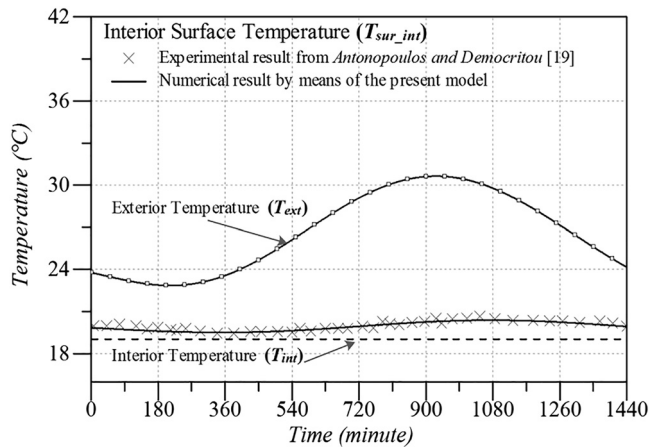


Fig. 2. Experimental validation of the model: Comparison of the numerical simulation result by means of the present model with the experimental result of Antonopoulos and Democritou [19]

exterior side of a 10-cm thick wallboard ( $T_{ext}$ ), while keeping a constant temperature on the other side of the wallboard ( $T_{int}$ ). Then, the exterior and interior surface temperatures of the wallboard ( $T_{sur\_ext}$  and  $T_{sur\_int}$ ) were measured.

In this study, the numerical simulation is carried out under real climate conditions.  $T_{ext}$  is given according to the sol-air temperature formulation that combines the effect of the outdoor temperature  $T_{out}$  and the global solar radiation  $G$  (Power).  $T_{ext}$  is given then as follows:

$$T_{ext} = T_{sa} = \left( T_{out} + \frac{\alpha \cdot G}{h_{ext}} \right) - \left( \frac{\varepsilon \cdot \Delta F}{h_{ext}} \right) \quad (8)$$

where  $\alpha$  is the solar absorptivity of the walls and roof. It was assumed equal to 0.6 that correspond to a medium-light colour. The last term of the equation is equal to 4 for horizontal surface (i.e. roof), and 0 for vertical surface (i.e. walls) [20]. The temperature  $T_{int}$  represents the indoor building condition, and it was considered as a constant value equal to 20 °C in winter, and at 26 °C based on the Moroccan building thermal regulation standard [21].

### 2.3. Climate zones and climate data sources

Morocco is a country of the subtropical zone of North-West Africa with a diversified climate. The Moroccan territory is divided into six climate zones. The study is carried out for six representative cities of the different climatic zones of Morocco [22, 23], namely:

- Tanger (Lat:35.74 °N, Long: –5.83 °E. Climate: Mediterranean hot)
- Fès (Lat: 33.93 °N, Long: –4.98°E. Climate: Mediterranean continental)
- Ifrane (Lat:33.5 °N, Long: –5.16 °E. Climate: Summer Humid temperate/Cold hiver)
- Marrakech (Lat:31.61 °N, Long: –8.03 °E. Climate: Hot semi-arid)

–Er-rachidia (Lat:31.93 °N, Long: –4.4 °E. Climate: Hot desert climate)

–Agadir (Lat: 30.38 °N, Long: –9.56 °E. Climate: Semi-arid.)

### 2.4. Current and future climate data

The typical year weather data are widely used by researchers and designers for building energy simulation purposes. It represents an average year of a climatological time period. Meteonorm is, among others, an international meteorological database that provides for solar engineering and building simulation applications at any desired location on the globe [24]. The standard weather file is generated based on the climatological periods (1961–1990 or 2000–2009) period for temperature and the climatological periods (1981–1990 or 1991–2010) for solar radiation. Besides, Meteonorm provides a future weather file for under the different climate change scenarios.

The future climate data are elaborated based on the special report on emissions scenarios of the International Panel on Climate Change (IPCC) [10]. Three principal scenarios have been included in Meteonorm: B1: Low GHG emissions scenario, A1B: Medium GHG emissions scenario, and A2: High GHG emissions scenario. The corresponding climate data are available for each decade from 2020 to 2100 and at every location in the globe.

In this work, the A1B GHG emission scenario of IPCC has been considered to generate future climate data for the 2040s (2040–2049) and 2060s (2060–2069). The A1B scenario is a balanced scenario based on the hypothesis of energy mixed, that is coherent with the Moroccan's strategy in the diversification of energy sources. Besides, the use of an historic data as baseline data seems to be outdated in 2020, and thus the A1B projected climate data for the 2020s was considered to approximate the current decade climate conditions.

### 2.5. Wall/roof structures

The choice of the wall and the roof material is made according to common building materials that are used in Morocco. Figure 3 presents the structure of the wall and

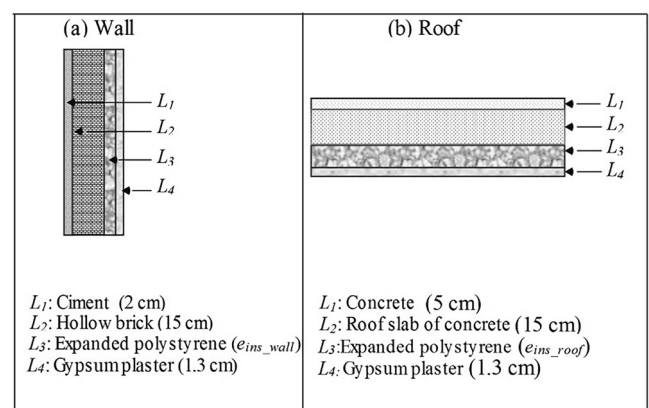


Fig. 3. Structures of wall and roof

Table 1. The U-factor value of the wall/roof and the appropriate insulation layer's thickness ( $e_{ins}$ ) for different climate zones

|                | U-value of wall  | $e_{ins\_wall}$ | U-value of roof  | $e_{ins\_roof}$ |
|----------------|--|-----------------|--|-----------------|
| Z1: Agadir     | $\leq 1.20$ ( $\text{w/m}^{-2}\cdot^{\circ}\text{C}$ ) | 0 cm            | $\leq 0.75$ ( $\text{w/m}^{-2}\cdot^{\circ}\text{C}$ ) | 6 cm            |
| Z2: Tangier    | $\leq 0.80$ ( $\text{w/m}^{-2}\cdot^{\circ}\text{C}$ ) | 2 cm            | $\leq 0.75$ ( $\text{w/m}^{-2}\cdot^{\circ}\text{C}$ ) | 6 cm            |
| Z3: Fes        | $\leq 0.80$ ( $\text{w/m}^{-2}\cdot^{\circ}\text{C}$ ) | 2 cm            | $\leq 0.65$ ( $\text{w/m}^{-2}\cdot^{\circ}\text{C}$ ) | 7 cm            |
| Z4: Ifrane     | $\leq 0.60$ ( $\text{w/m}^{-2}\cdot^{\circ}\text{C}$ ) | 5 cm            | $\leq 0.55$ ( $\text{w/m}^{-2}\cdot^{\circ}\text{C}$ ) | 9 cm            |
| Z5: Marrakech  | $\leq 0.80$ ( $\text{w/m}^{-2}\cdot^{\circ}\text{C}$ ) | 2 cm            | $\leq 0.65$ ( $\text{w/m}^{-2}\cdot^{\circ}\text{C}$ ) | 7 cm            |
| Z6: Errachidia | $\leq 0.80$ ( $\text{w/m}^{-2}\cdot^{\circ}\text{C}$ ) | 2 cm            | $\leq 0.65$ ( $\text{w/m}^{-2}\cdot^{\circ}\text{C}$ ) | 7 cm            |

roof. The thickness of the insulation layer is calculated to meet the minimum requirement as defined by the building thermal code for each climate zone in Morocco [21] (see Table 1).

### 3. RESULTS AND DISCUSSIONS

#### 3.1. Climate data overview

At first, a general overview of climate data generated by the *Meteonorm* for the 2020s, 2040s, and 2060s is given for the different climate zones in Morocco. Figures 4 and 5 depict the monthly mean temperature ( $T_{ext}$ ) and the monthly global solar radiation on horizontal surface ( $G_h$ ) in January and July. Obviously, an increase of  $T_{ext}$  is remarked over the future time period for climate zone. The most important increase of the  $T_{ex}$  is expected for Ifrane city. Indeed, compared to the 2020s, the monthly mean  $T_{ext}$  in January and in July are expected to increase, respectively, by 28% (+1.4 °C) and by 8.8% (+2 °C) in 2060s. While, the low percentage increase of  $T_{ext}$  would occur in the case of Agadir city. The monthly means  $T_{ext}$  in January and July are expected to increase, respectively, by 8% (+1.2 °C) and by 5.2% (+1.2 °C) when comparing the 2020s with the 2060s. As far as the global solar radiation on horizontal surface ( $G_h$ )

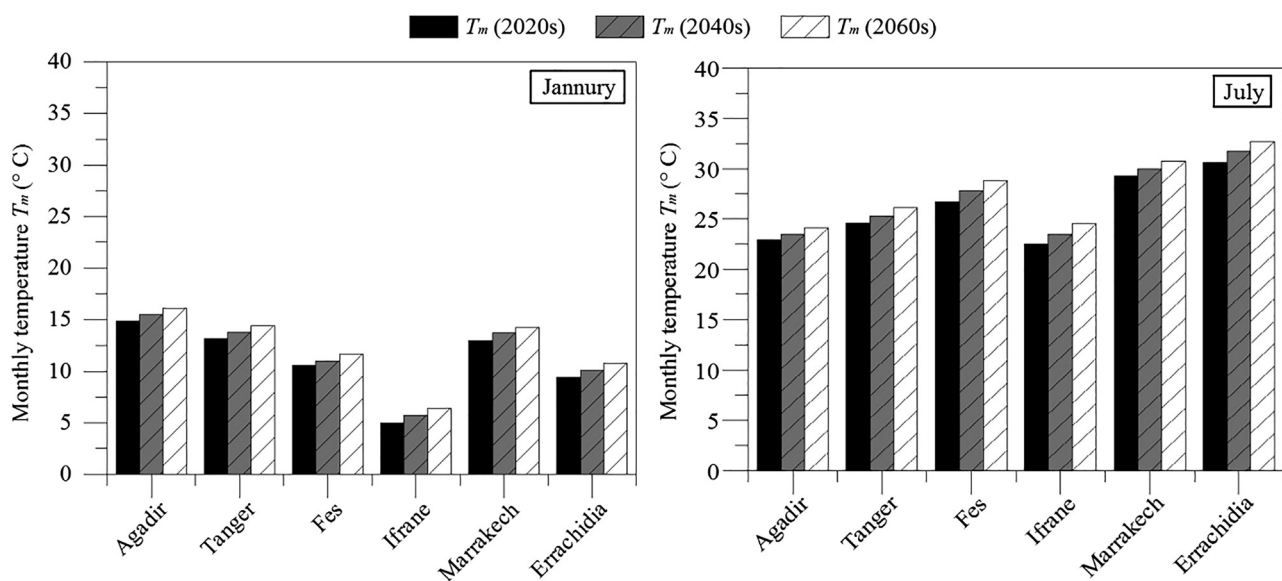
is concerned, it is intended to be more stable over time from the 2020s to the 2060s in different climate zones. The most significant variation is expected in January in Tangier city. In relation to 2020s, the  $G_h$  is likely to increase about 1.23% (+1 kWh/m<sup>2</sup>) by 2060s.

#### 3.2. Thermal performance assessment and analysis

The thermal performances of walls and roof under current and future climate conditions are presented and analysed for the different climate zones in Morocco. The months of January and July are chosen to represent typical winter and summer conditions, respectively.

**3.2.1. Current walls/roof thermal performance.** We will start by analysing the walls/roof thermal performance using the current climate data (2020s). Figure 6 presents the monthly winter heat loss ( $Q_{win}$ ) and summer heat gain ( $Q_{sum}$ ) per square meter of walls/roof. The red bars in the graph correspond to the summer heat gain that takes conventionally a positive value, while the blue bars represent the winter heat loss that takes conventionally a negative value.

Agadir and Tanger are coastal cities located respectively on the Atlantic Ocean and the Mediterranean Sea. These two cities have, among others, the mildest climate in Morocco

Fig. 4. Monthly mean temperature ( $T_{ext}$ ) in January and July

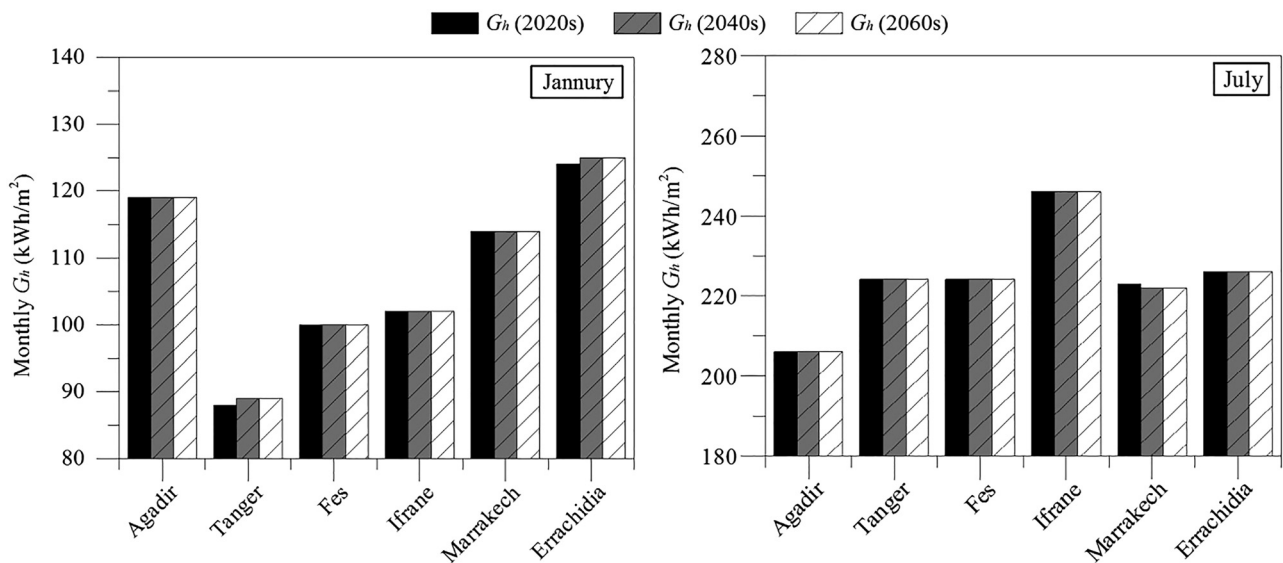


Fig. 5. Monthly global solar radiation on horizontal surface ( $G_h$ ) in January and July

throughout the whole year. So, the winter heat loss and summer heat gain are both limited. Errachidia city is characterized by a warm desert climate with cold winter and hot summer. That explains the important heat and cool load for January and July, respectively. Because of its higher elevation (+1665 m), Ifrane city's winter is quite cold in which the temperature can drop below zero degrees Celsius.  $Q_{win}$  of January is very important with an averaged value, for the total of the walls plus the roof, up to  $-18.9$  MJ. This value is still close to the one to that has been found in Fes city ( $Q_{win} = -16.1$  MJ), even though Fes city is characterized by a warmer winter condition compared to Ifrane city. This dissimilarity is due to the difference of the overall heat transfer coefficient (U-value) of the walls and roof. The Moroccan building thermal regulation defines the thickness of the insulation layer according to each climate zone condition. The insulation layers of the walls and roof used in the case of Ifrane, are thicker, respectively, by 3 cm and 2 cm than in the case Fes. That limits the heat loss through the walls and roof even in winter extreme conditions such as in Ifrane. Later during the summer season, this thermal resistance limits the heat gain from indoor to outdoor. Indeed, Ifrane summer heat gain is very limited and does not exceed, on average, 2.5 MJ for July.

**3.2.2. Future climate change projections.** The summer thermal heat loss ( $Q_{win}$ ) and winter heat gain ( $Q_{sum}$ ) of the walls and roof have been calculated for the 2040s and 2060s climate conditions. The intermediate A1B GHG emissions scenario is considered. In order to compare the thermal performance of walls/roof under the current climate and the future climate scenario, we present Fig. 7, the predicted percentage change ( $\Delta Q$  (%)) of  $Q_{win}$  and  $Q_{sum}$  in 2040s and 2060s compared to baseline climate (i.e. 2020s).

As was mentioned above, the months of January and July have been chosen to represent the winter and summer conditions.  $\Delta Q$  is calculated as follows:

$$\Delta Q(\%) = \left( \frac{Q(\text{Futur}) - Q(\text{Baseline})}{Q(\text{Baseline})} \right) \times 100 \quad (9)$$

The results showed that climate change affects differently the building envelope elements energy performance depending on the season. Indeed, climate change will positively affect the winter building performance by reducing  $Q_{sum}$ . While a negative impact is expected on the summer building performance through the reduction of  $Q_{win}$ . This result is still consistent with previous work outputs [6–13], given that the heat loss and heat gain through the walls and roof define mainly the heating and cooling energy consumption.

Other general observations can be summarized as follows:

- The intensity of the impact of climate change on thermal performances of walls/roof could be almost doubled between the two periods 2040s and 2060s compared to the 2020s.
- The impact of climate change is more visible in summer than in the cold season. The results presented that the current average walls/roof July heat gain is expected to increase of about 19.2–54.3% by the 2060s. This increase is offset by a general decrease in January heat loss during the cold season between  $-10.6$  and  $-20.6\%$ .
- By comparing the percentage of change in the outdoor temperature over the next 40 years and the corresponding change in the amount heat gain/loss, it is observed that climate change presents a multiplier effect on the summer building performance. Taking the case of Agadir city as an example, the average July heat gain could increase by 31.3% from the 2020s–2060s, while the corresponding expected increase of outdoor temperature does not exceed 5.2% (see Fig. 2). The same observation is also valid in the winter, while taking into consideration the opposite effect of climate change on the winter heat loss.
- Walls and roof with low U-values may not lead to taking advantage of climate change in the reduction of winter

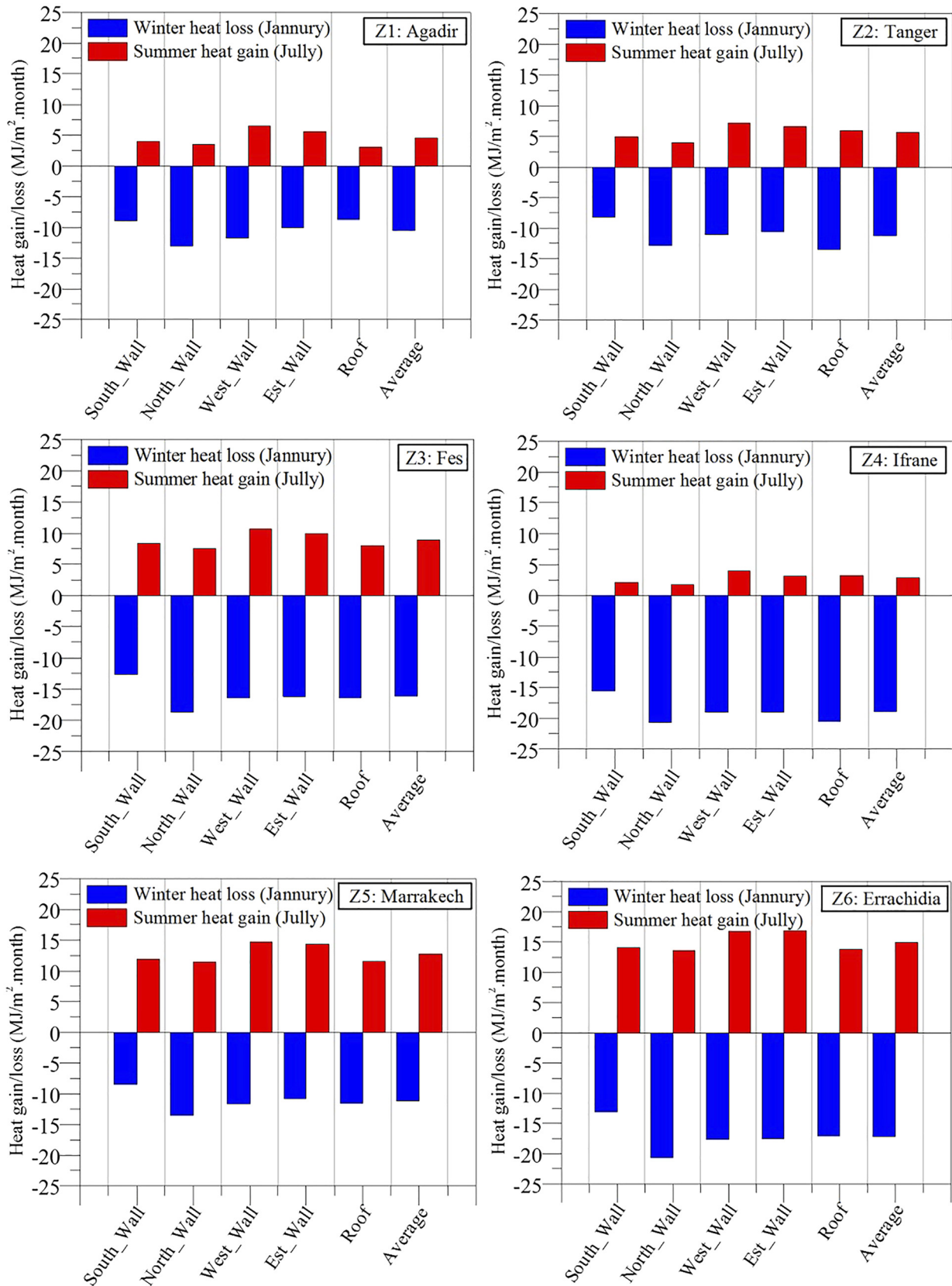


Fig. 6. Monthly winter heat loss ( $Q_{win}$ ) and summer heat gain ( $Q_{sum}$ ) of walls/roof for the 2020s



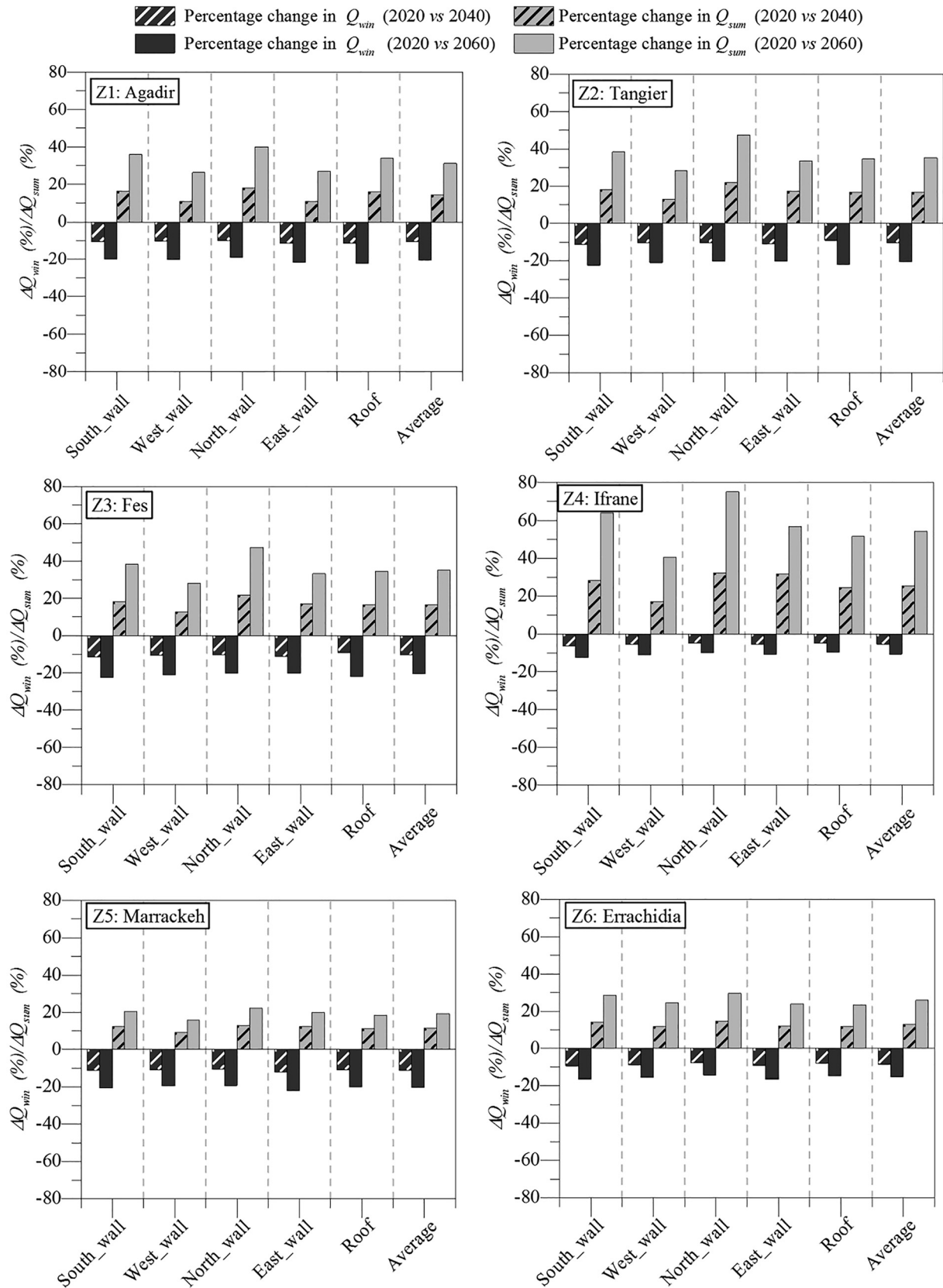


Fig. 7. Predicted change in January heat loss ( $\Delta Q_{win}$  (%)) and July heat gain ( $\Delta Q_{sum}$  (%)) compared to 2020s



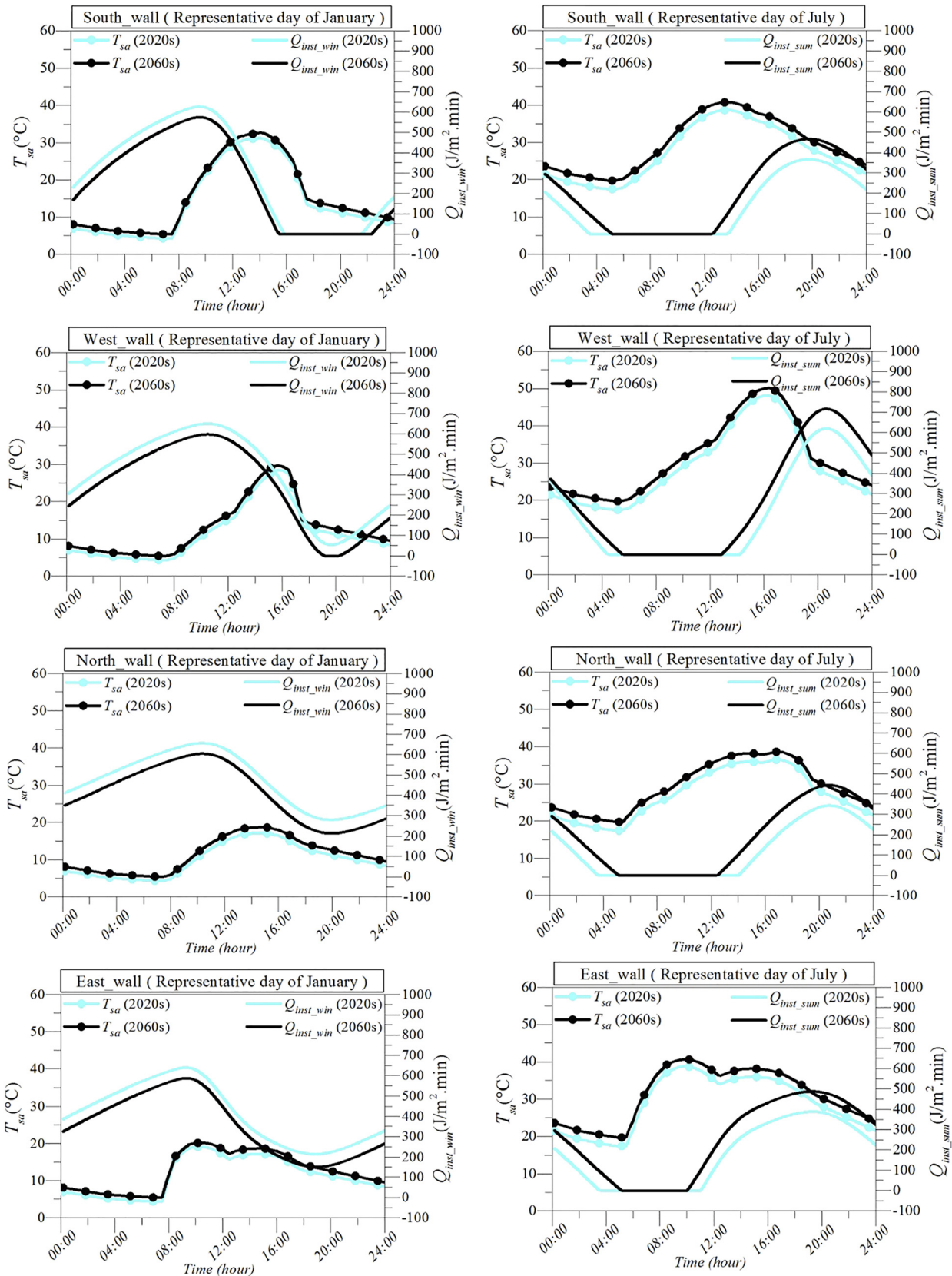


Fig. 8. Instantaneous variation of January heat loss ( $Q_{inst,win}$ ) and July heat gain ( $Q_{inst,sum}$ ) during a representative day of January and July, respectively



heat loss. This applies to the climate zone of Ifrane, which is characterized by a lower  $U$ -value. A slight decrease of the winter heat loss is expected ( $-10.6\%$ ) versus an important increase in the summer heat gain ( $+54.3\%$ ). This result is coherent with the outcomes of [13]. The study compared the heating energy demand of a residential building under the current and the 2050 climate conditions, while varying the values of coefficient  $U$ . The authors have found that lowering the  $U$ -value of opaque and transparent building envelope elements could limit the positive impact of climate change on the winter heating demand. We cite, for example, the obtained results for Naples city Italy, it was found that the reduction in the heating energy due to the effect of the climate pass from  $-31$  to  $\sim 0\%$  when decreasing the  $U$ -values of opaque envelope elements from  $1.25$  ( $\text{W}/\text{m}^{-2}\cdot^{\circ}\text{C}$ ) to  $0.15$  ( $\text{W}/\text{m}^{-2}\cdot^{\circ}\text{C}$ ).

- In winter, the positive effect of climate change is expected to be more important in mild and warmer climate as in the case of Agadir, Tangier, and Marrakech.
- In summer, the impact of climate change is expected to be more intense in colder climate zones as in the case of Ifrane city and Fes city.

With regards to wall orientation, the potential impact of climate change would be more balanced in winter between different wall facades, rather than in summer. As an example, in Fes city, the expected percentage decrease of  $Q_{win}$  by 2060s varies between  $-14.1$  and  $-15.8\%$  (Discrepancy of  $1.7\%$ ). On the other hand, the expected percentage increase of July  $Q_{sum}$  by 2060 varies between  $31.3$  and  $45.9\%$  (Discrepancy of  $14.6\%$ ). The highest and lowest percentage increases of the  $Q_{sum}$  over the next 40 years are expected, respectively, for the north-facing wall and the west-facing wall.

Further analysis can be done by comparing the instantaneous variation of  $Q_{win}$  and  $Q_{sum}$  during a representative day of January and July, respectively. The instantaneous variation of January heat loss ( $Q_{inst,win}$ ) and July heat gain ( $Q_{inst,sum}$ ) were obtained based on Eqs. 1(a) and 1(b). The case of Fes city is taken for example. The obtained results for the 2020s and the 2060s climate conditions are depicted in Fig. 8, together with the data of sol-air temperature ( $T_{sa}$ ).  $T_{sa}$  is expected to be higher in the 2060s compared to the 2020s due to the increase of the global temperature in the future decades. Consequently, as we can see in Fig. 8, the instantaneous values of  $Q_{inst,win}$  are lower in the 2060s compared to 2020s, while the instantaneous values of  $Q_{inst,sum}$  are higher in 2060s compared to 2020s. In July, the evolution of the  $Q_{inst,sum}$  follows the same direction to the  $T_{sa}$  with a certain delay time. This delay is due to the time required for the heat wave to propagate from the exterior wall surface to the interior wall surface. The peak day values of  $Q_{inst,sum}$  happen between 17h:00 and 21h:00 for all walls. The highest peak of  $Q_{inst,sum}$  occurs in the west-facing wall which has the highest peak value of  $T_{sa}$ . In January, the evolution of the  $Q_{inst,win}$  follows an opposite direction to the  $T_{sa}$  with also a delay time.  $T_{sa}$  begins to decline from the afternoon to reach its minimum peak value in the early hours of the morning. This decline is followed, with a delay time, by an increase of

the  $Q_{inst,win}$ . The peak day values of  $Q_{inst,win}$  occur between 21h:00 and 23h:00 according to the wall facade.

## 4. CONCLUSION

In this study, the thermal performance of the walls and roof over the next 40 years is evaluated and compared in Morocco under the 2020s, 2040s, and 2060s periods climate conditions. The summer heat gain and winter heat loss are used to assess the thermal performance of walls and roof. A representative month is used considered for each season. The future climate projections are based upon the medium GHG emissions A1B scenario.

The interpretation of the current and the expected future climatic data showed that in all climate zones of Morocco, there would be an increase in global warming due essentially to the increase of outdoor temperature rather than solar radiation. Consequently, an increase in the summer heat gain is expected in the future decades. In contrast, climate change would impact positively, although to a lesser extent, on the winter heat load by reducing heat loss. This reality forces us to think of an alternative design of the future building by focusing on the winter energy efficiency measures.

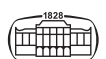
Furthermore, the results showed that the impact of climate change varies not only according to climate zone, but also according the building envelope element. Given that, at the present, the estimation of the standard heat transfer coefficient ( $U$ -value) is carried out commonly for all wall facades, and use a past climate data, it remains necessary to perform an adjustment of the calculation of the standard  $U$ -value coefficient. Further studies are required to determine the ideal  $U$ -value by each facade wall and by taking into account future climate conditions.

The assessment of the thermal performance of walls and roof under future climate conditions was done based on a hypothesis on the climate change scenario. Indeed, the main objective of this kind of work was not to estimate exactly the thermal performance indicators of the building envelope elements under future climate, but to approach these indicators according to the hypothesis adopted in the study. The results of this study are still inconclusive and depend on the uncertainties over future changes in the Moroccan climate; however, they represent a starting point for Moroccan building designers to integrate the effect of climate change in future building constructions.

*Conflict of interest:* Authors declare no conflict of interest regarding the publication.

## NOMENCLATURE

|           |  |
|-----------|--|
| $C$       | Thermal capacitance ( $\text{J}/^{\circ}\text{C}^{-1}$ )                               |
| $cp$      | Specific heat capacity ( $\text{J}/\text{kg}^{-1}\cdot^{\circ}\text{C}$ )              |
| $e_{ins}$ | Thickness of insulation layer (cm)   |
| $G_h$     | Global solar radiation on horizontal surface ( $\text{kWh}/\text{m}^{-2}$ )            |
| $h$       | Convective heat transfer coefficient ( $\text{W}/\text{m}^{-2}\cdot^{\circ}\text{C}$ ) |



|                               |  |
|-------------------------------|--|
| $L$                           | Material layer   |
| $l$                           | Thickness of wall/roof (m)   |
| $L_1 \dots L_K$               | Layer 1... layer $K$   |
| $Q_{win}/Q_{sum}$             | Winter heat loss/summer heat gain (MJ)   |
| $Q_{win\_inst}/Q_{sum\_inst}$ | Instantaneous heat loss/gain during the winter/summer ( $J/m^{-2} \cdot min$ ) |
| $R$                           | Thermal resistance ( $^{\circ}C/W$ )   |
| $S$                           | Layer surface area ( $m^2$ )   |
| $T$                           | Temperature ( $^{\circ}C$ )  |
| $t$                           | Time (minute)  |
| $U$                           | Heat transfer coefficient ( $W/m^{-2} \cdot ^{\circ}C$ )                       |

## GREEK SYMBOLS

|            |   |
|------------|---|
| $\Delta t$ | Time step (minute)                                  |
| $\Delta X$ | Sub-layer thickness (cm)                            |
| $\alpha$   | Solar absorptivity (-)                              |
| $\lambda$  | Thermal conductivity ( $W/m^{-1} \cdot ^{\circ}C$ ) |
| $\rho$     | Density ( $Kg/m^{-3}$ )                             |

## SUBSCRIPTS

|                     |                                   |
|---------------------|-----------------------------------|
| $ext/int$           | Exterior/interior                 |
| $j$                 | Node index                        |
| $out$               | Outdoor                           |
| $sur\_ext/sur\_int$ | exterior surface/interior surface |

## REFERENCES

- [1] UNFCCC, "What is the United Nations framework convention on climate change?," 1994. [Online]. Available: <https://unfccc.int/process-and-meetings/the-convention/what-is-the-united-nations-framework-convention-on-climate-change>. Accessed: Oct. 21, 2020.
- [2] United Nations, "Kyoto protocol to the United Nations framework convention on climate change," 1998.
- [3] United Nations, "Adoption of the Paris agreement," Paris, 2015.
- [4] IPCC, "Fifth assessment synthesis report-climate change," Gian-Kasper Plattner, 2014.
- [5] IPCC, "Buildings," in *Climate Change 2014: Mitigation of Climate Change*, 2014, pp. 671–738.
- [6] T. Frank, "Climate change impacts on building heating and cooling energy demand in Switzerland," *Energy Build.*, vol. 37, pp. 1175–85, Nov. 2005. <https://doi.org/10.1016/j.enbuild.2005.06.019>.
- [7] X. Wang, D. Chen, and Z. Ren, "Assessment of climate change impact on residential building heating and cooling energy requirement in Australia," *Building Environ.*, vol. 45, no. 7, pp. 1663–82, Jul. 2010. <https://doi.org/10.1016/j.buildenv.2010.01.022>.
- [8] A. F. Hamlet, S. Y. Lee, K. E. B. Mickelson, and M. M. Elsner, "Effects of projected climate change on energy supply and demand in the Pacific Northwest and Washington State," *Climatic Change*, vol. 102, no. 1–2, pp. 103–28, May 2010. <https://doi.org/10.1007/s10584-010-9857-y>.
- [9] A. Invidiata and E. Ghisi, "Impact of climate change on heating and cooling energy demand in houses in Brazil," *Energy Build.*, vol. 130, pp. 20–32, Oct. 2016. <https://doi.org/10.1016/j.enbuild.2016.07.067>.
- [10] IPCC, "IPCC Special report on emissions scenarios," 2000.
- [11] U. Berardi and P. Jafarpur, "Assessing the impact of climate change on building heating and cooling energy demand in Canada," *Renew. Sustain. Energy Rev.*, vol. 121, p. 109681, Apr. 2020. <https://doi.org/10.1016/j.rser.2019.109681>.
- [12] M. K. Nematshoua, A. Yvon, O. Kalameu, S. Asadi, R. Choudhary, and S. Reiter, "Impact of climate change on demands for heating and cooling energy in hospitals: An in-depth case study of six islands located in the Indian Ocean region," *Sustain. Cities Soc.*, vol. 44, pp. 629–45, Jan. 2019. <https://doi.org/10.1016/j.scs.2018.10.031>.
- [13] E. Rodrigues and M. S. Fernandes, "Overheating risk in Mediterranean residential buildings: Comparison of current and future climate scenarios," *Appl. Energy*, vol. 259, p. 114110, Feb. 2020. <https://doi.org/10.1016/j.apenergy.2019.114110>.
- [14] D. H. W. Li, L. Yang, and J. C. Lam, "Impact of climate change on energy use in the built environment in different climate zones – A review," *Energy*, vol. 42, no. 1, pp. 103–12, Jun. 2012. <https://doi.org/10.1016/j.energy.2012.03.044>.
- [15] World Health Organisation, "Climat et Santé: Profil de Pays-2015 Maroc," 2015.
- [16] W. Cramer, J. Guiot, M. Fader, J. Garrabou, J. Gattuso, A. Iglesias, M. A. Lange, P. Lionello, M. C. Llasat, S. Paz, J. Peñuelas, M. Snoussi, A. Toreti, M. N. Tsimplis, and E. Xoplaki, "Climate change and interconnected risks to sustainable development in the mediterranean," *Nat. Clim. Change*, vol. 8, no. 11. Nature Publishing Group, pp. 972–80, 01-Nov-2018. <https://doi.org/10.1038/s41558-018-0299-2>.
- [17] Y. Kharbouch, L. Ouhsaine, A. Mimet, and M. El Ganaoui, "Thermal performance investigation of a PCM-enhanced wall/roof in northern Morocco," *Build. Simul.*, vol. 11, no. 6, pp. 1083–93, 2018. <https://doi.org/10.1007/s12273-018-0449-5>.
- [18] R. Idchabani, "Contribution à l'efficacité énergétique du bâtiment résidentiel au Maroc: modélisation et optimisation de l'isolation thermique," Université mohammed V Agdal, 2014.
- [19] K. A. Antonopoulos and F. Democritou, "Experimental and numerical study of unsteady non-periodic wall heat transfer under step, ramp and cosine temperature perturbations," *Int. J. Energy Res.*, vol. 18, no. 6, pp. 563–79, 1994. <https://doi.org/10.1002/er.4440180602>.
- [20] American society of heating refrigerating and air-conditioning engineers, in *2009 ASHRAE Handbook Fundamentals*, Inch-Pound. Atlanta: ASHRAE, 2009.
- [21] Moroccan Agency for Energy Efficiency, "Moroccan building thermal regulation code," 2010.
- [22] M. C. Peel, B. L. Finlayson, T. A. McMahon, M. C. Peel, B. L. Finlayson, and T. A. M. Updated, "Updated world map of the Köppen-Geiger climate classification," *Hydrol. Earth Syst. Sci.*, vol. 11, no. 5, pp. 1633–44, 2007.
- [23] Météo Maroc, "Moroccan climate zones," 2010.
- [24] Meteotest, "Meteonorm 7." Bern, Switzerland, 2014.

**Open Access.** This is an open-access article distributed under the terms of the Creative Commons Attribution-NonCommercial 4.0 International License (<https://creativecommons.org/licenses/by-nc/4.0/>), which permits unrestricted use, distribution, and reproduction in any medium for non-commercial purposes, provided the original author and source are credited, a link to the CC License is provided, and changes – if any – are indicated.

